Mechanical Systems and Signal Processing 85 (2017) 809–826

Contents lists available at ScienceDirect

Mechanical Systems and Signal Processing

journal homepage: www.elsevier.com/locate/ymssp

# Audio signal analysis for tool wear monitoring in sheet metal stamping

Indivarie Ubhayaratne[a,*], Michael P. Pereira[b], Yong Xiang[a], Bernard F. Rolfe[b]

[a] School of Information Technology, Deakin University, Locked Bag 20000, Geelong, VIC 3220, Australia
[b] School of Engineering, Deakin University, Locked Bag 20000, Geelong, VIC 3220, Australia

ARTICLE INFO

*Keywords:*
Galling
Tool wear
Sheet metal stamping
Condition monitoring
Audio signal analysis
Blind signal extraction

ABSTRACT

Stamping tool wear can significantly degrade product quality, and hence, online tool condition monitoring is a timely need in many manufacturing industries. Even though a large amount of research has been conducted employing different sensor signals, there is still an unmet demand for a low-cost easy to set up condition monitoring system. Audio signal analysis is a simple method that has the potential to meet this demand, but has not been previously used for stamping process monitoring. Hence, this paper studies the existence and the significance of the correlation between emitted sound signals and the wear state of sheet metal stamping tools. The corrupting sources generated by the tooling of the stamping press and surrounding machinery have higher amplitudes compared to that of the sound emitted by the stamping operation itself. Therefore, a newly developed semi-blind signal extraction technique was employed as a pre-processing technique to mitigate the contribution of these corrupting sources. The spectral analysis results of the raw and extracted signals demonstrate a significant qualitative relationship between wear progression and the emitted sound signature. This study lays the basis for employing low-cost audio signal analysis in the development of a real-time industrial tool condition monitoring system.

## 1. Introduction

Sheet metal stamping is the most frequently used primary manufacturing method for mass-production of automotive body and structural components. Since, global automotive production exceeds 60 million vehicles per year, and there are over one hundred sheet metal components on average in each car, this potentially has a very significant number of applications even for just the automotive industry alone. Hence, even a small improvement could be highly influential to the product quality and cost efficiency. The increasing trends towards advanced- and ultra-high strength steels (AHSS and UHSS) in the automotive industry for continued vehicle light-weighting has increased forming forces, die wear and galling and, therefore, has resulted in premature die failures. These faults are difficult to predict at the design stage and may lead to expensive tool replacements and additional costs due to poor part quality, machine downtime and unscheduled maintenance [1]. Hence, stamping tool condition monitoring is a timely need. The aim of implementing a monitoring system is to achieve uninterrupted production and prevent the adverse consequences described. However, current techniques for assessing tool wear and part quality rely on manual visual inspection of formed part surface quality or the tool surface condition. These methods only provide information about the state of the tooling after the wear has become severe and, therefore, can be too late to prevent production downfall. Hence, it is a non-trivial requirement to have a system for online

* Corresponding author.
*E-mail addresses:* kubhayar@deakin.edu.au (I. Ubhayaratne), michael.pereira@deakin.edu.au (M.P. Pereira), yong.xiang@deakin.edu.au (Y. Xiang), bernard.rolfe@deakin.edu.au (B.F. Rolfe).

http://dx.doi.org/10.1016/j.ymssp.2016.09.014
Received 25 February 2016; Received in revised form 7 July 2016; Accepted 10 September 2016

monitoring of tool condition that can provide the early detection of tool wear and identification of the current tool state.

Du et al. [2] presented a comprehensive review on the sensing and online monitoring techniques for sheet metal stamping processes. Other earlier reviews and research articles [3–6] provide evidence of progress in this area, but still demonstrate the current need for a high-performance condition monitoring system. Tonnage or force monitoring has been the most popular [7,8] while other commonly used sensors include acceleration [9], proximity, optical [5,6], and acoustic emission [10,11]. Du. et al. [2] reviewed strain, acceleration, force and proximity sensors and argued that force and proximity sensors could be effective, but the sensor cost is too high. Acceleration sensors are cost effective, but very high computational power is necessary to convert the signal into useful information. Strain and acoustic emission sensor signals are rich in wear information, but can be difficult to install, since they must be mounted on the tool or sheet surfaces [12]. Despite this research, there is still an unmet demand from manufacturing industries for a low-cost easy to set up condition monitoring system which is capable of detecting the onset of wear.

Audible acoustic sensors (microphones) have a higher potential to meet this demand compared to other acoustic sensor types - such as vibration (acceleration) and acoustic emission sensors - due to their low-cost, non-disruption to the ongoing operation and simplicity in sensor placement and setup. However, the high sensitivity to background noise has hindered the employment of microphones in real applications. Audio has been employed in many other manufacturing applications, except stamping, such as diesel engine injection monitoring [13], rolling element bearing defect detection [14] and monitoring of machining/cutting operations such as turning [15–17], micro milling [18,19], and drilling [20,21]. Downey et al. [22] conducted audio analysis to study a single point machining operation in an environment where no other machine operations occurred at the same time. Unfortunately, this will not be the case in a real production environment. Additionally, this study and other research works [12,23] were founded on the characteristic that experienced operators can differentiate the good quality and degraded process conditions by hearing changes in the emitted sound. Depending on the manufacturing process and application examined, the emitted audio signal characteristics in both time and frequency domains can significantly vary as evidenced by the wide range of literature findings. For example, Eneyew et al. [20] observed a decreasing trend of sound amplitude with the number of holes drilled, while Downey et al. [22] detected an increasing trend in amplitude with the number of machining cycles. A shift in signal energy from a lower frequency range to a higher frequency range is observed with wear formation in micro-milling operations [12] and in turning operations [15]. However, in metal cutting it has been shown that higher amplitude signal peaks appear in the upper frequency range for sharp tools and in the lower frequency range for worn tools [24].

However, these existing techniques focus on identifying few distinct wear levels or faults such as slug, misfeed, or tool breakage. Furthermore, to the authors' best knowledge, no work in the literature has examined the use of audio sensors for progressive wear monitoring in sheet metal stamping. One of the reasons for this may be that even an experienced stamping process operator cannot distinguish the wear state of the tools by relying on his/her hearing. Hence, it is still unknown if emitted audio carries any information about wear progression of the stamping tools. To ensure this, it is necessary to obtain the audio emitted by stamping. However, it is not straightforward to isolate the stamping signal since most of the industrial production lines use mechanical presses with progressive die sets or transfer press systems, which integrate several operations – such as piercing, trimming, feeding, clamping, restrike, etc. –within a single stamping press stroke. Our recent work [25] has shown that these additional operations may emit higher intensity sound signals compared to stamping, making it difficult for the human ear to recover the stamping signal.

Therefore, it is particularly useful to determine firstly if the emitted sound from the stamping operation contains any useful information related to wear progression. If this is the case, sound-based condition monitoring systems would be highly preferred by manufacturing industries due to the advantages discussed earlier. In the studies discussed above, several techniques have been developed/employed for data processing based on fast fourier transform (FFT) analysis, cepstrum, wavelet analysis [26], singular spectrum analysis (SSA) [16,17], and Hilbert Huang transform (HHT) [27,28]. Speech recognition systems [23], pattern recognition systems [24], neural network systems [29], and support vector machines [16] have been used in the decision making phase. Nevertheless, there is a lack of robust methods which consider the disturbances by other processes/components of the machine and background signals. This point is a key impediment for application to the real production environment, and therefore, there is a need for techniques to recover information from corrupted sensor signals.

Blind signal separation (BSS) is an effective technique capable of recovering unobserved source signals from observed mixtures without any information of the mixing system [30–33]. BSS first emerged as a biological problem in 1982 and then evolved to successful usage in several applications such as communication, audio processing (speech and music) and image processing [34]. BSS also has been employed in mechanical applications, including rotating machinery condition monitoring [35,36], fault detection [37] and condition monitoring of manufacturing processes like milling [38–40]. Among the BSS techniques for manufacturing process monitoring, Shao et al. [38] and Shi et al. [39] focused on single channel source separation, using power signals and audio signals respectively. Both of these studies face computational complexity due to the selection of a single sensor to deal with higher sensor cost and installation inconveniences. As initial studies, they have conducted experimental analysis on the extreme conditions (i.e. sharp tool condition against severe tool breakage) and have noted the need for future investigations into minor tool breakages or tool wear. The direct usage of above techniques for our application is hindered because the BSS algorithm development depends on original source characteristics, which differ from application to application.

Hence, a blind signal separation technique, appropriate for the application, should be developed. Since the knowledge of original signal characteristics and the mixture model is unavailable, system parameterization was necessary and was previously conducted by Ubhayaratne et al. [25]. In this analysis, the audio signals generated by the stamping operation were modeled as a BSS system and a simple semi-blind signal extraction technique was developed. This is not a final signal separation solution. However, it served the purpose of recovering the stamping signal so that it could be employed in studying the correlation between wear progression and audio emissions. However, in [25] this signal extraction technique was tested only on four distinct tool/operation conditions: (i)

unworn dies with lubrication; (ii) unworn dies without lubrication; (iii) severely worn dies with lubrication; and (iv) and severely worn dies without lubrication. This technique has not been tested on continuous wear progression. However, the ability to identify changes in the signals during continuous wear progression is a critical step in developing a condition monitoring method. The current study investigates the correlation between audio emissions and continuous wear progression, which is bridging the gap between existing research. Also, in [25] qualitative analysis of the time domain waveform and the quantitative analysis of time domain signal features, such as maximum amplitude and the RMS value, were employed. Even though time domain features were capable of distinguishing distinct wear levels, they fail to demonstrate a significant pattern with continuous wear progression. Thus, frequency domain analysis was introduced in the current study.

This paper provides the first steps towards the aim to develop a real-time industrial stamping tool condition monitoring system. A mechanical press with a channel forming tool set was used for the experiments. Stamping was started with unused die corner radii inserts and run continuously until the die radii surfaces showed severe wear. At this point, the surface quality of the stamped parts was unacceptable, and the process would typically be aborted in a real production environment. Conventional microphones were used for recording the emitted sound. These microphone recordings were a mixture of the signal of interest and other corrupting signals due to the nature of the process, and so the stamping related audio signal was recovered using the technique in [25]. Spectral analysis was conducted on raw and extracted signals, and the observations are discussed in correlation with the wear conditions that are qualitatively observed on the formed channel part surfaces, both visually and via profilometry measurements.

The overall contribution of this study compared to existing work can be summarized as follows:

i. Study of signal behaviour with continuous wear progression, instead of specific tool defects or few distinct wear levels, which has not been studied before for sheet metal stamping processes.
ii. The new design of the experimental setup to generate the data specific to the condition explained in i. The experiment was carefully designed to generate progressive wear with near-production industrial stamping conditions, preventing other faulty conditions such as misfeed, slug or intermittent wear conditions.
iii. Application of frequency domain analysis instead of time domain waveform analysis because the time domain analysis employed in [25] does not show a significant correlation with continuous wear progression.

The rest of the paper is organized as follows. Sections 2.1–2.3 explains the stamping equipment, materials and the data acquisition setup used for the experiments, respectively. Section 2.4 describes the conducted experiments in detail, and Section 2.5 details the surface quality inspection using profilometry. Section 3.1 presents the signal extraction technique used as a pre-processing step and Section 3.2 gives the details on the spectral analysis conducted on raw and processed data to compare the signal behaviour with wear progression. The results obtained by the application of the proposed technique and four other existing techniques are presented in Section 4. Section 5 provides a discussion of the results and future work, and the concluding remarks are in Section 6.

## 2. Experimental outline

This experiment aims to determine if the simple audio analysis could be employed to detect the die wear and galling, and the primary objectives of the experimental design were to:

a) closely replicate the industrial stamping operation and near-production process conditions;
b) generate progressive wear, preventing other possible faults such as slug, misfeed, and intermittent wear conditions.

### 2.1. Stamping equipment

The experiments were conducted using a semi-industrial sheet metal stamping test setup, as shown in Fig. 1. This process produces channel-shaped parts (Fig. 1(c)), using a progressive die set and single-action mechanical press. This test has been specifically designed to closely replicate the conditions experienced during continuous stamping production, with emphasis on the wear conditions at the die radii, as described in detail previously by Pereira et al. [41,42]. The geometric, process and material parameters used resemble a typical wear-prone automotive sheet metal stamping operation and near-production process conditions. The important parameters and conditions are summarized in Table 1. All the conditions were kept constant throughout the trials.

Due to the use of a progressive die set, there are also clamping, piercing and trimming operations that occur during each stroke. Additionally, the sheet metal coil is fed by an automated feeder through an uncoiler and straightener. Although these operations are not the focus of condition monitoring, a brief explanation of these is given below, since the signal pre-processing technique was developed based on this knowledge. The schematic shown in Fig. 1(b) does not reflect the exact positioning of the tools and does not show all of the other operations, so the sequence of operations varies from this due to the physical placement of the tools. The piercing punches (#08) and stamping dies (#02) are mounted to the upper plate (#09), which is attached to the press ram and is moved vertically by the action of the press motor and crank. During the downward movement of the ram, the following points describe the most important operations relative to this study and the order in which they occur:

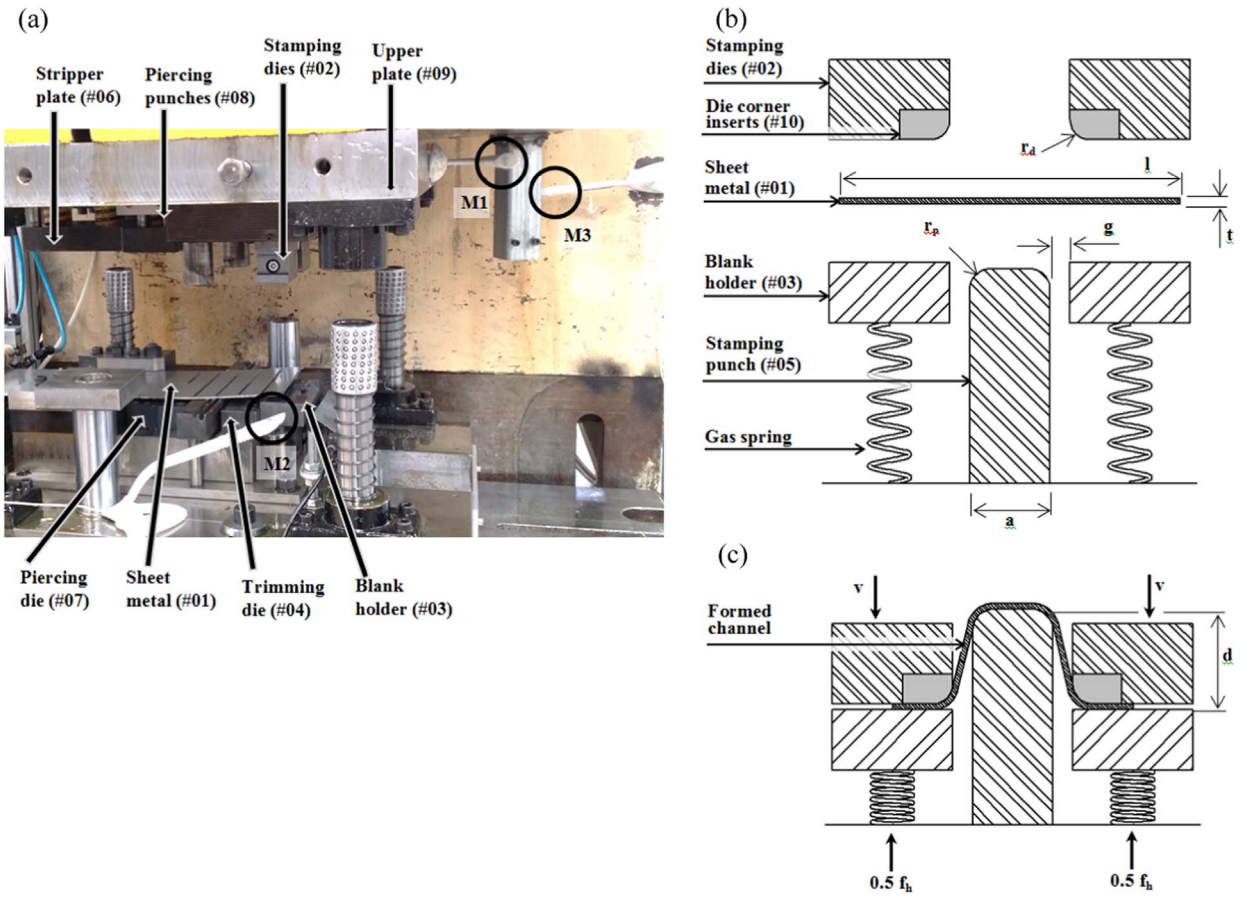


**Fig. 1.** (a) The sheet metal stamping press tool setup and the microphone placement around the tooling; (b) Schematic of the channel forming wear test at the start of each cycle; (c) The u-shaped formed channel.

**Table 1**
Process parameters.

| | |
|---|---|
| Punch width, a | 30 mm |
| Draw depth, d | 40 mm |
| Average blank holder force, $f_h$ | 28 kN |
| Die-to-punch gap, g | 2.3 mm |
| Blank length, l | 150 mm |
| Die corner radius, $r_d$ | 5 mm |
| Punch corner radius, $r_p$ | 5 mm |
| Blank thickness, t | 1.6 mm |
| Blank width, w | 26 mm |
| Press stroke length | 203 mm |
| Press rate | 32 $min^{-1}$ |

1. The sheet metal strip (#01) is clamped between the stamping dies (#02) and blank holder (#03) at approximately 50 mm before bottom dead centre (BBDC).
2. The small tabs at the ends of the sheet metal strip are trimmed by the shearing action of the sharp edge of the stamping die (#02) and the trimming die (#04) at ~45 mm BBDC. This causes the approximately rectangular section of sheet metal blank to be separated from the rest of the coil.
3. The sheet metal blank contacts the top of the stamping punch (#05) at ~40 mm BBDC, and is then formed over the punch with further movement of the stamping dies (#02) downward.
4. The sheet metal strip (#01), which is located prior to the forming operation and is still attached to the sheet metal coil, is clamped between the stripper plate (#06) and the piercing die (#07) at ~7 mm BBDC.
5. Near the bottom of the press stroke, at ~3 mm BBDC, the piercing punches (#08) contact the sheet metal strip (#01) and begin punching two long thin slots (approximately 4 mm×75 mm) into the sheet metal. This operation produces the approximately

rectangular strips of sheet metal (150 mm long×26 mm wide), with the small tabs at the ends, described in Point 2 above.
6. At bottom dead centre (BDC), the stamping operation is complete. The press ram then begins its ascent for the upwards part of the stroke.
7. The feeding operation begins during the upward part of the stroke at approximately 100° before top dead centre (BTDC). The sheet is fed 30 mm during each cycle.

The mechanical press operates continuously at 32 strokes per minute. At this press rate, the punch speed is approximately 300 mm/s at the beginning of the forming operation and reduces to 0 mm/s at the end of the 40 mm forming stroke at BDC, as governed by the geometry and kinematics of the press and tooling system and the press crankshaft rotational speed.

### 2.2. Materials

The die corner inserts (#10) are removable, permitting interchange of the wearing surfaces. These die inserts were manufactured from AISI D2 grade tool steel. They were rough milled to obtain the approximate shape; then through hardened to 60HRC, and then precision ground. To achieve an accurate surface profile and the desired surface finish, the die radius region was finished via manual polishing. These preparation processes are conventional practice in the stamping industry [43]. However, in this case, extra care was taken during each of the manufacturing steps to ensure a profile tolerance of ± 0.05 mm over the die radius insert surfaces that are in contact with the blank material, as described in our previous experimental work on stamping wear [44].

The blank material is a low-carbon hot-rolled steel grade and has a nominal thickness of 1.6 mm. This steel is designated as XF300 by the supplier and it conforms to the AS/NZS 1594 specification. In the rolling direction, the yield strength and ultimate tensile strength (UTS) are 321 MPa and 485 MPa, respectively, and the total uniform elongation is 19.2%, as determined from uniaxial tensile tests.

The blank material was lightly lubricated with anti-corrosive oil, designated as Ferrocote 366 K2 50 by the supplier. The lubricant was applied via an automatic lubrication process, using oiled rollers, before entering the tooling. The die insert holders, blank holder and punch were made from hardened AISI D2 tool steel that was plasma-nitrided and PVD-coated with TiCN to ensure no wear.

### 2.3. Data acquisition setup

The signals emitted by only three operations - trimming, stamping and piercing (described in Points 2, 3 and 5 in Section 2.1) - contribute to the audio mixtures employed in the analysis. This is because only those signals have significant signal strengths and also occupy overlapped time frames. Therefore, for the data acquisition, three microphones were employed in order to satisfy a general assumption of blind signal separation algorithms to have an equal or larger number of outputs than the number of input sources. The complete setup consists of:

1. Three microphones (directionality: omnidirectional, sensitivity: −62 dB -/+3 dB, frequency range: 20 Hz to 16 kHz, operating voltage: 1 V-10 V), as labelled in Fig. 1(a). Microphone M1 was mounted on the moving upper plate (#09) of the tooling close to the stamping dies. Microphone M2 was mounted on the stationary bottom plate close to the trimming die (#04), and M3 was mounted on the stationary press frame.
2. A position sensor was used to record the starting point of each stroke, indicating when the crank of the mechanical press is at the top dead centre (TDC) during each cycle.
3. A National Instruments USB-6009 data acquisition system. Four analog channels of this eight channel data acquisition system were used to record the three microphone outputs and the position signal.
4. Thinkpad Lenovo laptop with National Instruments Signal Express software.

The microphone placement presented in Fig. 1(a) was chosen based on the spatial distribution of the tools generating the three main sound sources. Data was collected at 12 kHz rate. This was limited due to the maximum cumulative sampling rate of the data acquisition card.

### 2.4. Methodology for stamping tests

The experiment began with unused die inserts, prepared with the method described in Section 2.2. The channel parts were formed continuously and their surfaces were visually inspected regularly until severe scratches appeared in the middle of the sidewalls of the stamped parts. The existence of these scratches indicates failure of the stamping process due to severe wear on the die inserts. This method of manual visual inspection was similar to the method described by Lilljengren et al. [45], during sheet metal stamping wear studies conducted at Volvo Cars. After the experiment, 3D profilometry measurements of the channel part surfaces were obtained.

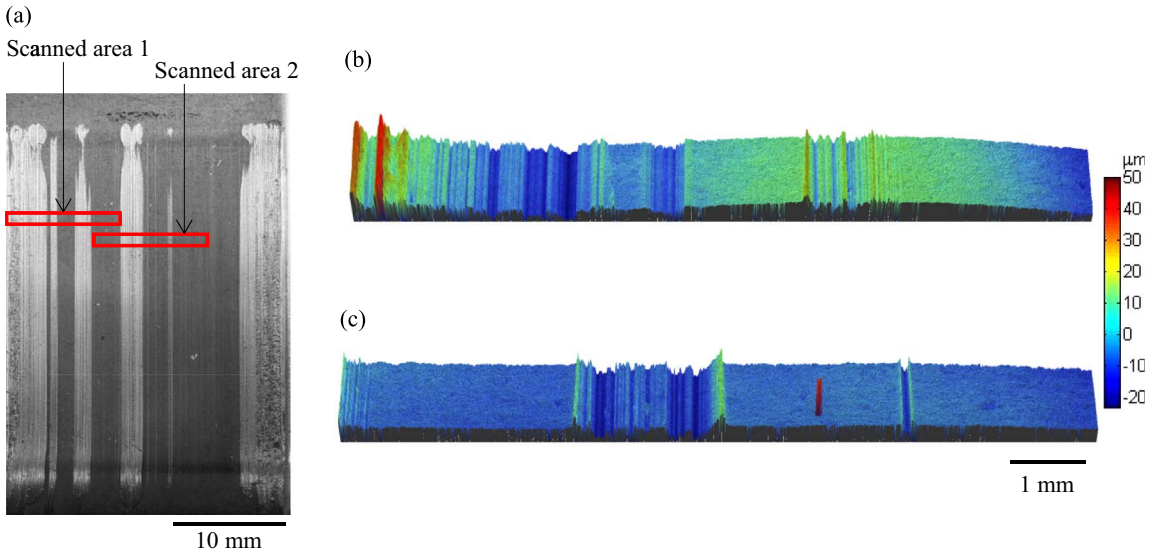


**Fig. 2.** (a) Detailed view of sidewall of a formed channel part, after 1300 parts formed, showing the areas where the 3D profilometry scans were obtained; (b) 3D profilometry scan of scanned area 1; (c) 3D profilometry scan of scanned area 2.

### *2.5. Profilometry*

Two 10×1 mm areas of each part, covering across most of the sidewall of the parts, were scanned using a Veeco 3D optical profilometer (model name: Contour GT), as shown in Fig. 2(a). The edge of the sidewall (scanned area 1) was selected since the initial scratches on the parts started to appear from the edge. Scanned area 2 was selected to cover the scratches due to wear formed on the middle of the sidewall of the parts, since the decision to terminate the stamping operation (i.e. failure of the dies) is based on the scratches observed in this area. The sidewalls of the channel parts are not completely flat and have a slight curvature in both directions. Therefore, after obtaining the scanned profile, 'tilt and curvature removal' was applied to the measurement data from within the profilometer software [46]. 'Tilt removal' removes the residual tilt that occurs during a measurement in order to make inclined samples level. The 'curvature' is the shape proportional to the second derivative of the surface data and its removal allows the observation of surface features instead of the dominant curved shape. Examples of the 3D profiles of the scanned areas 1 and 2, after tilt and curvature removal, are presented in Fig. 2(b) and (c). Fig. 2(D) profile plots were obtained from these 3D profilometry scans and studied with regards to the wear progression.

## 3. Signal processing

Stamping operations, in general, would generate noisy audio because this operation is conducted following, or at the same time as, several other manufacturing operations. Hence, a semi-blind signal extraction algorithm, which is detailed in Section 3.1, was employed to extract the audio associated with the stamping operation only. Then spectral analysis was conducted on raw and extracted data in order to study the correlation between the wear formation of stamping dies and the audio emissions.

### *3.1. Signal extraction technique*

The audio signals emitted within the time window where stamping is active were used for the analysis. The three main audio sources – trimming, stamping and piercing (described in Section 2.3) – share similar frequency and amplitude ranges. Hence, the recordings obtained from the microphones are signal mixtures, which cannot be directly used for condition monitoring or easily separated by simple filtering. For this reason, the blind signal separation approach was employed.

Initially, four specially designed machine cycles were run (trials A to D) with different combinations of operations in order to obtain temporal information about each operation. This was achieved by disabling particular operations programmatically or removing the corresponding tools physically. The operations that were active during each of the four trials are described in Fig. 3(a) and the audio signals recorded by microphone M1 are shown in Fig. 3(b). Trial A represents the press motor running with none of the operations active and hence it can be considered as a measurement for additive noise. The time windows where each of the operations are active – $T_1$, $T_2$, and $T_3$ – are marked in Fig. 3(b).

The signals emitted by piercing and trimming are recorded independently within the time periods $T_1$ of trial B and $T_2$ of trial C respectively. However, the signal generated by stamping – i.e. during the period $T_3$ of trial D – could not be isolated by the procedure of disabling operations or removing tooling. Hence, a data extraction algorithm was developed based on the following blind signal separation model:

(a)

| Trial | Trimming | Piercing | Stamping | Noise |
|---|---|---|---|---|
| A | - | - | - | ✓ |
| B | - | ✓ | - | ✓ |
| C | ✓ | ✓ | - | ✓ |
| D | ✓ | ✓ | ✓ | ✓ |

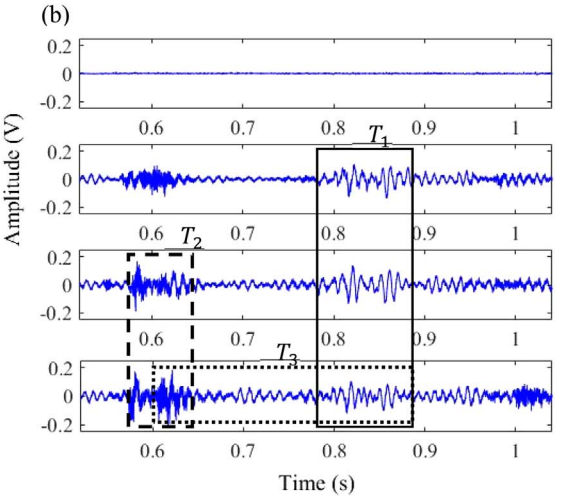


**Fig. 3.** Trials A – D: (a) the active press operations, (b) microphone M1 recordings with the time windows of each operation. ▬ Time window where piercing is active ($T_1$); ▬ ▬ Time window where trimming is active ($T_2$); ..... Time window where stamping is active ($T_3$).

$$Y(n) = AX(n) + W(n) \tag{1}$$

where $Y(n) = [y_1(n) + y_2(n) + y_3(n)]^T$ is the channel output vector, $X(n) = [x_1(n) + x_2(n) + x_3(n)]^T$ is the input vector, $W(n) = [w_1(n) + w_2(n) + w_3(n)]^T$ is the additive noise vector, and $A$ is the 3×3 instantaneous mixture matrix whose column vectors are $a_1$, $a_2$, $a_3$. The superscript $^T$ denotes the transpose, and $n$ denotes the time instant. The mixture matrix can be assumed to be constant throughout the experiment due to the steady sensor placement and tool locations.

Two vectors proportional to the first two columns of matrix $A$ were obtained using eigenvalue decomposition of the noise free autocorrelation matrices of the channel output vectors of the trials that had piercing and trimming operations occurring alone - i.e. time periods $T_1$ of trial B, and $T_2$ of trial C respectively [25]. The steps of the signal extraction technique development are summarized below.

**Case 1.** :

Consider the signals active within the time period $T_1$ of trial B and define

$$Y^{(1)}(n) = AX^{(1)}(n) + W(n) \tag{2}$$

where (1) refers to the signals considered in Case 1. Since only $x_1(n)$ is active during $T_1$, (2) can be simplified to

$$Y^{(1)}(n) = a_1 x_1(n) + W(n) \tag{3}$$

The microphone outputs are proportional to the column $a_1$ at every time instant $n$, in the absence of noise. Hence, a vector proportional to $a_1$ can be obtained from $\frac{1}{N_1}\sum_{n=0}^{N_1-1} Y(n)$, where $N_1$ is the number of samples during $T_1$. In the general noisy case, a vector proportional to $a_1$ can be derived using eigenvalue decomposition of the output autocorrelation matrix after removing the noise contribution, by deducting the noise autocorrelation matrix. Define the input autocorrelation matrix $R_{XX}$ as

$$R_{XX} = \langle X(n)X^H(n)\rangle \tag{4}$$

and the autocorrelation function $\rho_{ii}$as

$$\rho_{ii} = \langle x_i(n)x_i^*(n)\rangle \tag{5}$$

where the superscript $H$ denotes the complex conjugate operator, and $\langle\bullet\rangle$ denotes the time averaging operator defined as

$$\langle x_i(n)x_i^*(n)\rangle = \lim_{n\to\infty}\frac{1}{N}\sum_{n=0}^{N-1} x_i(n)x_i^*(n) \tag{6}$$

where $N$ is the number of samples. Then, the output autocorrelation matrix in Case 1 can be obtained as $R_{YY}^{(1)} = \left\langle Y^{(1)}(n)Y^{(1)^H}(n)\right\rangle$. From (2) and (4), it follows

$$R_{YY}^{(1)} = AR_{XX}^{(1)}A^T + R_{WW}R_{YY}^{(1)} = AR_{XX}^{(1)}A^T + \sigma_w^2 I_3 \tag{7}$$

where $R_{WW}$ is the autocorrelation matrix of additive noise, and $\sigma_w^2$ is the noise variance and equals to the smallest eigenvalue of $R_{YY}^{(1)}$ and $I_3$ is the 3×3 identity matrix. From (3) and (5); (7) can be reduced to

$$R_{YY}^{(1)} = a_1 \rho_{11} a_1^T + \sigma_w^2 I_3 \tag{8}$$

and

$$R'_{YY} = R_{YY}^{(1)} - \sigma_w^2 I_3 \tag{9}$$

Obtain the eigenvector $v_1$ corresponding to the largest eigenvalue of $R'_{YY}$ and from (8) and (9) it can be concluded that $v_1$ is proportional to column$a_1$.

**Case 2:.** :

Consider the signals active within the time period $T_2$ of trial C and define

$$Y^{(2)}\left(n\right) = a_2 x_2\left(n\right) + W(n) \tag{10}$$

where (2) refers to the signals considered in Case 2. It follows

$$R_{YY'}^{(2)} = A R_{XX}^{(2)} A^T + \sigma_w^2 I_3 R_{YY}^{'} = R_{YY'}^{(2)} - \sigma_w^2 I_3 \tag{11}$$

In a similar manner, it can be shown that the eigenvector $v_2$ – corresponding to the largest eigenvalue of $R'_{YY}$, which is the noiseless output autocorrelation matrix in Case 2 – is proportional to column $a_2$.

Let $V=\left[v_1, v_2\right]$. Then vector $v_3$ from the null space of $V$ will be orthogonal to the columns $a_1$ and $a_2$. Without loss of generality, we can say that the probability of $v_3 \perp a_3$ is zero.

**Case 3:. :**

Consider time period $T_3$ of trial D, which is the general press operation. Hence, by multiplying the channel output vector by $v_3^T$, an estimate for $x_3(n)$ can be obtained.

$$v_3^T \cdot Y^{(3)}\left(n\right) = v_3^T \cdot A X^{(3)}\left(n\right) + v_3^T \cdot W(n) \tag{12}$$

where (3) refers to the signals considered in Case 3. Since $v_3 \perp a_1, a_2$, (12) can be simplified to

$$v_3^T \cdot Y^{(3)}\left(n\right) = \alpha x_3(n) + v_3^T \cdot W(n) \tag{13}$$

where $\alpha$ is a scalar introduced due to the common scalar ambiguity problem of the BSS algorithms. In this step, minimum-mean-square-error (MMSE) equalization [47] was employed to alleviate the impact of the noise. Then one can obtain an estimate for $x_3(n)$, as $\bar{x}_3\left(n\right) = v'^T_3 \cdot Y^{(3)}\left(n\right)$ up to a scalar, where $v'_3$ is MMSE equalization vector.

### 3.2. Data analysis

#### 3.2.1. Raw signal analysis

During the series of stamping tests, the operations and formed channels of seven distinct parts with different wear levels were selected as comparison points for the complete spectral analysis. At each comparison point, spectral analysis of the average of the waveforms generated by ten consecutive stamping operations was conducted in order to reduce any bias in the part selection, due to the part-to-part variation in the signals. Each frequency spectrum in Section 3.3 is divided into 4096 frequency bins. For studying the sound emitted by all 1500 channel parts, a simple aggregate spectral ratio approach was employed [22] to obtain a single quantitative measure representing the complete spectra corresponding to each part. This value is referred to as the 'relative cumulative spectral power index' (RCSPI), which is the cumulative frequency domain magnitudes of the signal corresponding to each part, divided by that of the first part. The initial comparison was conducted on the overall bandwidth. Secondly, band power analysis was conducted to understand how the signal behaves with wear progression in different frequency regions. For this, the complete frequency scale was divided into six distinct bands of width of 1 kHz, with the aim to identify the bands richest with the tool wear related information.

#### 3.2.2. Extracted signal analysis

The algorithm described in Section 3.1 was then applied to the raw audio recordings, in order to remove the signal contribution from the other processes of the stamping press and allow the change in the stamping signal with wear progression to be observed clearly. This algorithm selects the time window occupied by stamping in each stroke and outputs the extracted signal, which is the audio emitted by the stamping operation only. Then the signal analysis mentioned in the above section was repeated for the extracted signals.

## 4. Results and discussion

### 4.1. Visual inspection

Beginning with the unused die inserts, a total of 1500 parts were stamped until failure of the die insert was judged. The progression of the scratches on the sidewalls of the parts, due to wear of the die insert, is summarized by the photographs shown in Fig. 4. The analysis in this study focussed on the sidewalls on one side of the stamped channels, which contacted the left side die insert. When the test was stopped at 1500 parts, severe scratches were not evident on the other side of the stamped channel. This variation in the wear progression is often observed, due to the inherent variation in wear rate of processes dominated by adhesive wear as a result of the distinct initiation and rapid growth stages [48].

Part numbers 1, 100, 200, 500, 1000, 1300 and 1500 were selected as sample points with different wear levels. A gap of at least 100 parts was chosen to allow a significant difference in wear level to be observed. Initial scratches were evident on the edges of the sidewalls of the parts after 200 pieces were formed, as shown in Fig. 4(c). The severity and area of the scratches on the sidewalls gradually increased with the number of parts formed. After approximately 500 pieces were formed, the scratches became more severe and spread towards the middle of the sidewall (Fig. 4(d)). Complete failure of the die insert was judged to occur after 1500 pieces were formed, due to the existence of scratches across the entire sidewall surface, as shown in Fig. 4(g).

For industrial applications, it is appreciated that the number of pieces formed for tool steel die inserts are expected to be at least one order of magnitude higher than that exhibited during these semi-industrial tests – i.e. at least tens of thousands of pieces formed prior to maintenance or replacement of the die inserts. Prior to conducting the tests, it was known that the chosen combination of stamping tool and sheet materials, process conditions, tool geometry and lack of special lubrication, would result in a system that is highly prone to wear and galling. These conditions were chosen deliberately due to the costly and time-consuming nature of performing such wear tests and to ensure that the data could be collected reliably over a practical time frame. The results and outcomes of this work, in terms of the audio signal analysis, are still valid and relevant to longer time-scale tests because the observed wear mechanisms compare well with those experienced in industry during lower wear rate conditions.

### 4.2. 2D contour profiles of profilometry scans

The 2D profilometry contour profiles across the sidewall surfaces of the stamped channels after tilt and curvature removal are plotted in Fig. 5. As shown in Fig. 5(a), the edge of the surface of part 100 already shows some changes compared to the reference surface profile of the unworn first part, which was not perceptible to the naked eye during visual inspection. Scratches at the middle of the sidewall are evident in the 2D profiles at approximately part number 1000, and spread over the sidewall to a greater extent in part 1500 (Fig. 5(b)), correlating well with the visual observations in Fig. 4. The sidewall images and the 2D contour profiles clearly show a steady increase in the wear level with the number of parts formed, due to increases in severity, depth, number and area of the scratches observed. However, there is currently no reliable quantitative measurement for the severity of the wear on the die by examining the part surfaces. This will be the subject of future research.

### 4.3. Data analysis results

#### 4.3.1. Unprocessed audio analysis results

This section presents the analysis of the raw audio waveforms generated during the stamping of the channel parts. Fig. 6(a) presents the power spectral density of the microphone M1 signal for each of the seven parts shown in Fig. 4. The low-frequency signals shown in Fig. 6(a) are stronger and the details in the higher-frequency region are unclear due to the lower magnitude. Therefore, the frequency spectra were plotted within the 1.8–6 kHz range in Fig. 6(b), eliminating the high-magnitude peaks in the low-frequency range which do not show any correlation to the wear formation. Upon visual observation, the spectra show an

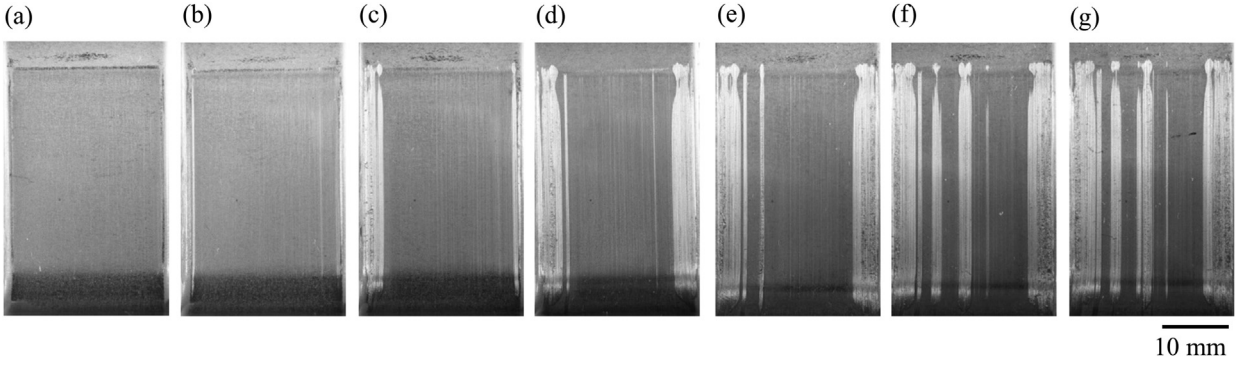


**Fig. 4.** Sidewalls of selected formed parts: (a) part 1, (b) part 100, (c) part 200, (d) part 500, (e) part 1000, (f) part 1300, (g) part 1500.

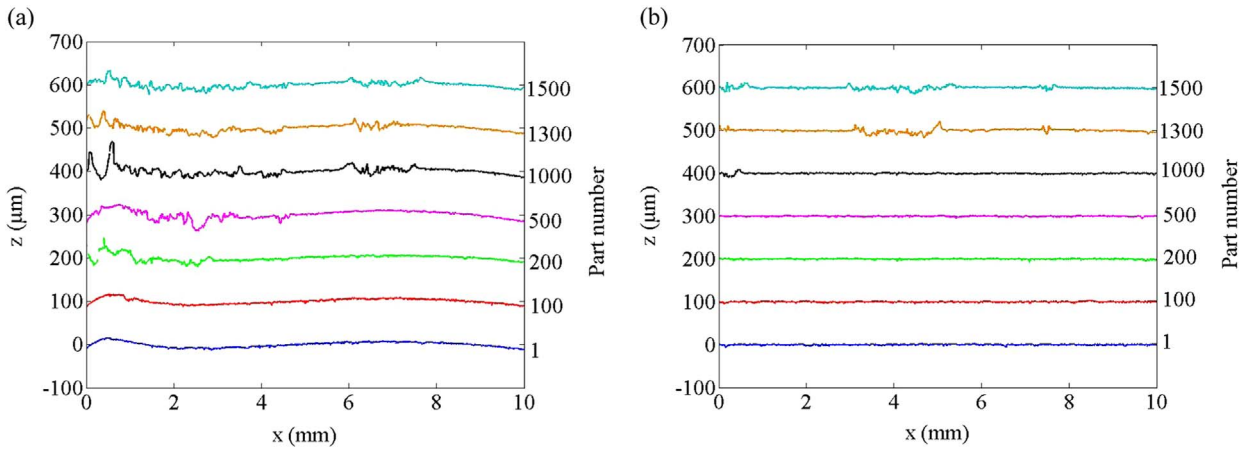


**Fig. 5.** The 2D profiles of each channel part within (a) scanned area 1 and (b) scanned area 2.

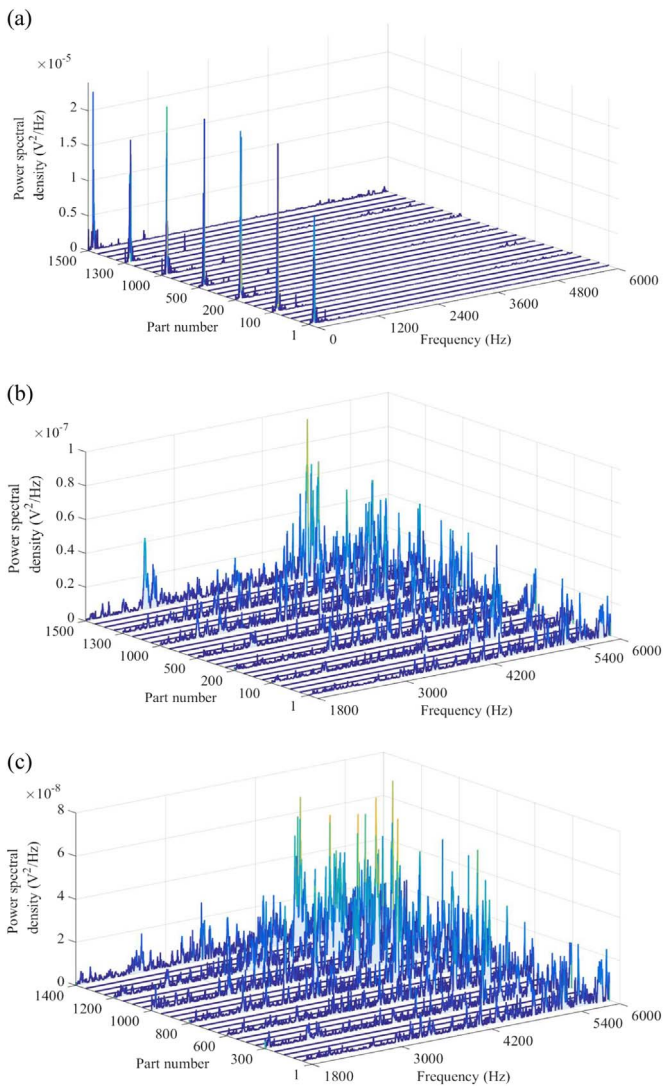


**Fig. 6.** : Spectral density of the raw microphone M1 signal: for parts 1, 100, 200, 500, 1000, 1300 and 1500 over (a) the complete bandwidth and (b) 1.8–6 kHz range, and (c) for parts 1, 300, 600, 800, 1000, 1200 and 1400 over 1.8–6 kHz range.

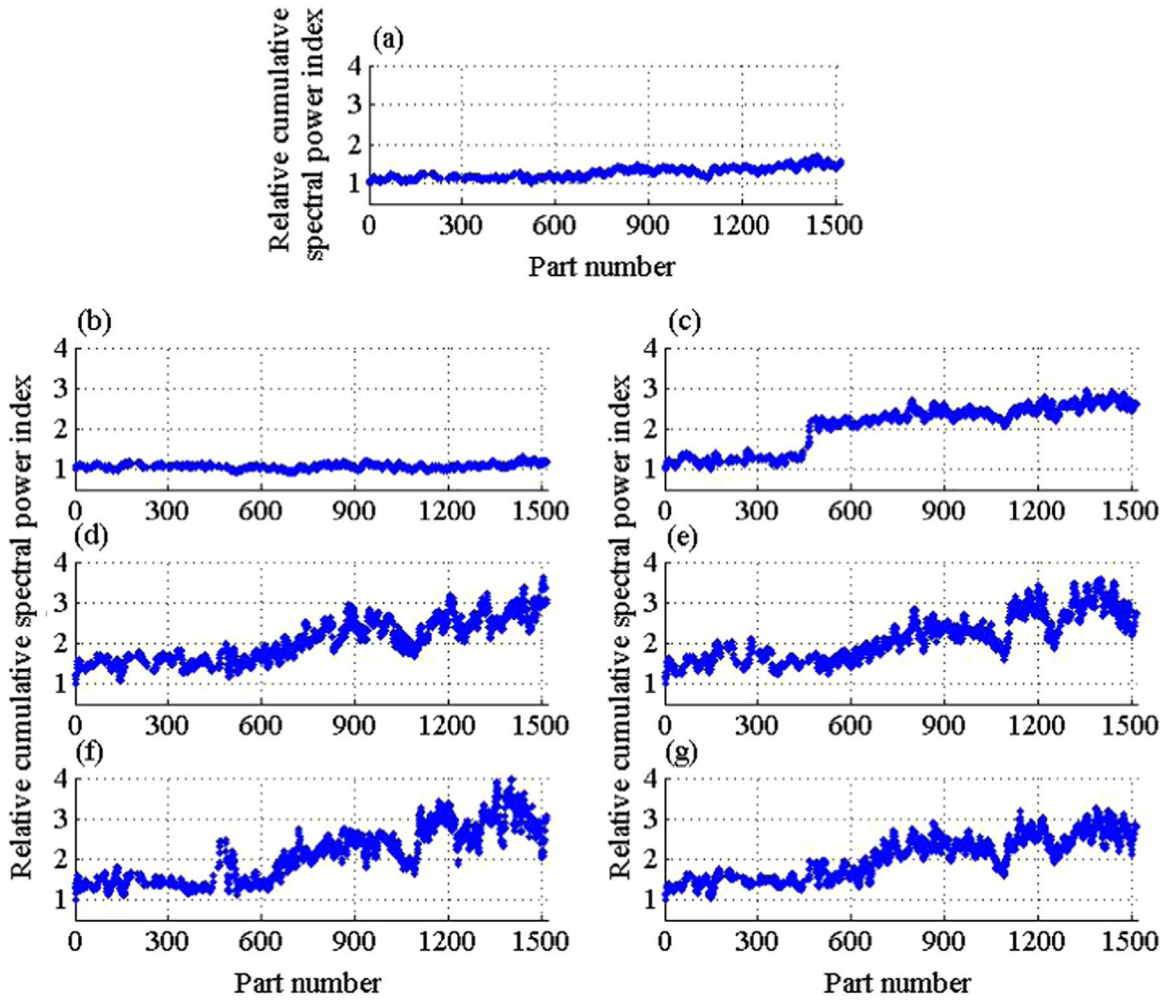


**Fig. 7.** The RCSPI values of the raw microphone M1 output within (a) complete bandwidth (0–6 kHz), (b) 0–1 kHz, (c) 1–2 kHz, (d) 2–3 kHz, (e) 3–4 kHz, (f) 4–5 kHz, and (g) 5–6 kHz bands.

increment in magnitude from the set of parts with low wear (1–500 parts) to the set of parts with high wear (1000–1500 parts). However, the difference in spectra is not significant within each set of parts. For an unbiased comparison, similar analysis was conducted for the signals generated by a second set of parts - parts 1, 300, 600, 800, 1000, 1200 and 1400 – and a similar behaviour was observed, as shown in Fig. 6(c).

The RCSPI signal for each part within the complete bandwidth are presented in Fig. 7(a). Fig. 7(b)–(g) present the power indices calculated within 1 kHz wide distinct frequency bands. The complete bandwidth analysis shows an approximately increasing trend, but is less obvious compared to some of the distinct bands. The RCSPI value appears almost steady within the 0–1 kHz band. In the 1–2 kHz band, a sudden jump of the index was observed at approximately the 500th part, but afterward, the index was approximately steady and did not show a strong link with wear progression. The frequency bands within the 2–6 kHz range show a clear increasing trend and the slope of the trend is higher after the 500th part. This can be correlated with the visual inspection and profilometry profiles, where the scratches due to wear became severe and spread inward approximately after 500 parts were formed. It can be seen that for the 2–6 kHz bands, the RCSPI curves exhibit more fluctuation from approximately 700 parts onward. This can be explained by the nature of the adhesive wear (galling) phenomena experienced on the tool surfaces. Galling involves the initiation, growth and removal of lumps of adhered sheet material at discrete points on the die surface. This non-continuous nature of the wear process results in fluctuations in the part surface quality (as can be seen when examining the surfaces of a large number of the parts formed), and hence fluctuations in the audio emissions, as shown in Fig. 7. The authors attribute the large changes in the higher frequency bands for RCSPI observed at approximately 1100 and 1250 parts to this same behaviour. The data in this region was examined carefully; the experiments ran continuously, no errors or issues were observed in the microphones and the data acquisition setup which can be evidenced by the consistent noise levels measured.

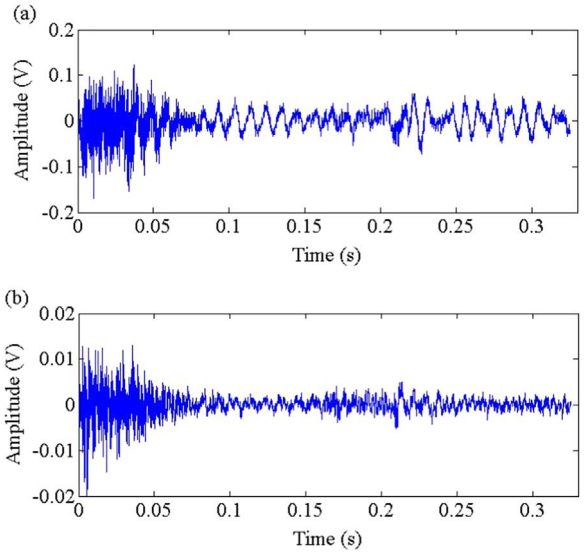


**Fig. 8.** (a) Signal mixture recorded by microphone M1; (b) extracted signal using proposed algorithm, for part number 1.

### *4.3.2. Extracted signal analysis results*

Fig. 8 presents the input and output of the signal extraction technique described in Section 2.6.1. The signal extraction technique has removed the audio signals generated by background processes and has recovered the unobserved information associated with the stamping operation from the observed signal mixtures.

Fig. 9 presents the similar analysis results to that of Fig. 6, but for the extracted signals. The low-frequency content, which is dominant in the raw microphone output spectra in Fig. 6(a), is reduced in the extracted signal spectra in Fig. 9(a). However, the magnitudes of the peaks in the frequency bins from 0 to 1.2 kHz still do not show any pattern over the wear progression. In contrast, the higher frequency range (2–6 kHz), shows a clear increasing trend in the magnitudes with the number of parts formed, which was not visible in the raw microphone signal analysis. The plots corresponding to parts 1000, 1300 and 1500 have stronger signal power. This can be correlated with the level of wear – i.e. the increased number and severity of the scratches seen in the photographs (Fig. 4) and the 2D surface profile plots (Fig. 5). This is particularly evident in the middle of the sidewalls after 1000 pieces were formed. Examining the magnitude of the spectra within the 1.8–6 kHz range (Fig. 9(b) and (c)) shows that the first part starts with an almost flat spectrum. The number and height of the peaks observed in the spectrum then gradually increase with increasing number of parts stamped. Although the increasing trend in audio signal strength is qualitatively visible in the raw audio data in Fig. 6, it is clearer and more consistently increasing in the extracted signals in Fig. 9. This observation can be linked with the fact that even an experienced stamping press operator is unable to distinguish the worn and unworn tool conditions by hearing the emitted sound, since the useful characteristics are concealed in the audio mixture.

### *4.3.3. Comparison analysis*

In this section, four existing techniques were applied to the audio data emitted by sheet metal stamping to compare their suitability in detecting continuous wear formation.

In [25] Ubhayaratne et al. combined semi-blind signal extraction technique with time-domain analysis for detecting the correlation with four distinct wear/process conditions. Fig. 10 presents the results of the same analysis applied to our current data set, which is collected during continuous wear progression. The RMS value and the maximum absolute peak amplitude show some increasing trend with the increase of the wear level, but this trend is less steady and less significant compared to the spectral analysis presented in Fig. 7. That is because the time domain features do not show a significant variation unless the wear level has a significant difference.

Sari et al. [49] observed the frequency distribution of the vibration signal with and without punching and identified the frequencies excited by the punching operation. They used the designated frequency/frequency range as the feature to be correlated with the different wear levels. The frequency distribution of the audio signals when the press was run with and without stamping (trials D and C explained in Section 3.1 respectively) is presented in Fig. 11. Two consecutive press runs were observed to make sure the pattern we discuss is consistent. The two pairs of frequency distributions did not demonstrate a significant difference, because the audio emitted by trimming, piercing and stamping processes share almost overlapping frequency ranges. However, frequency regions (I) 3100 – 3200 and (II) 5050 – 5150 Hz shown in Fig. 11 can be identified as having an association to the stamping operation to some extent. The audio signals within these regions were observed for four selected channel parts (Part 1, Part 500, Part 1000, and Part 1500) and the results are presented in Fig. 12. No obvious patterns can be identified in these results, as opposite to the vibration analysis results observed by Sari et al. [49]. Therefore, it was impractical to pick up the audio frequencies excited by the

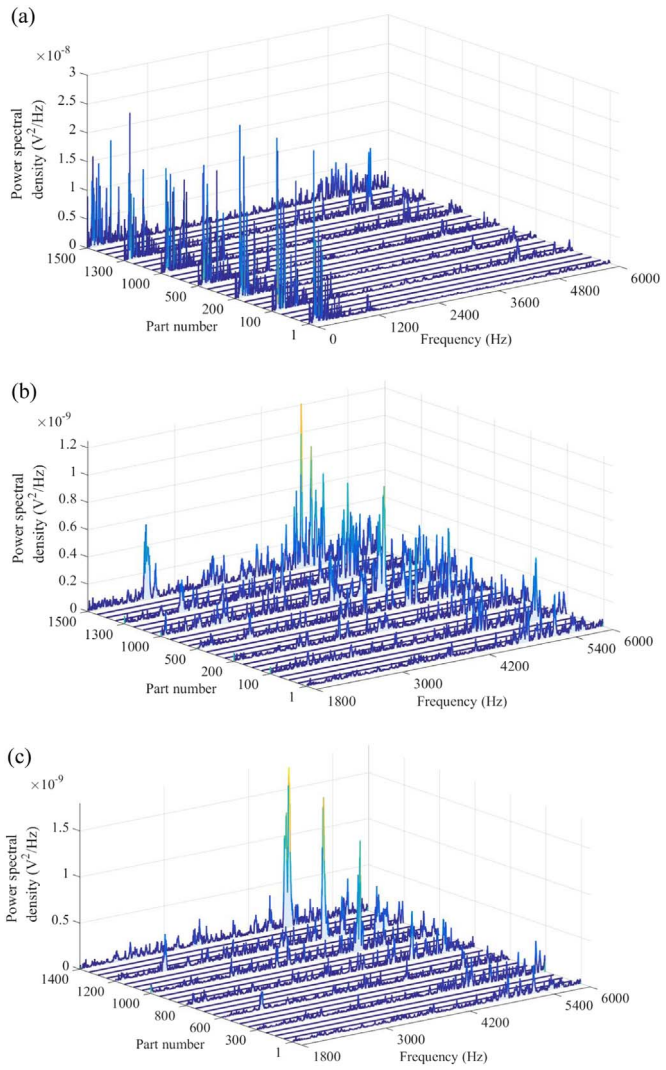


**Fig. 9.** Power spectral density of extracted signal: corresponding to parts 1, 100, 200, 500, 1000, 1300 and 1500 over (a) complete bandwidth and (b) 1.8–6 kHz range, and (c) corresponding to parts 1, 300, 600, 800, 1000, 1200 and 1400 over 1.8–6 kHz range.

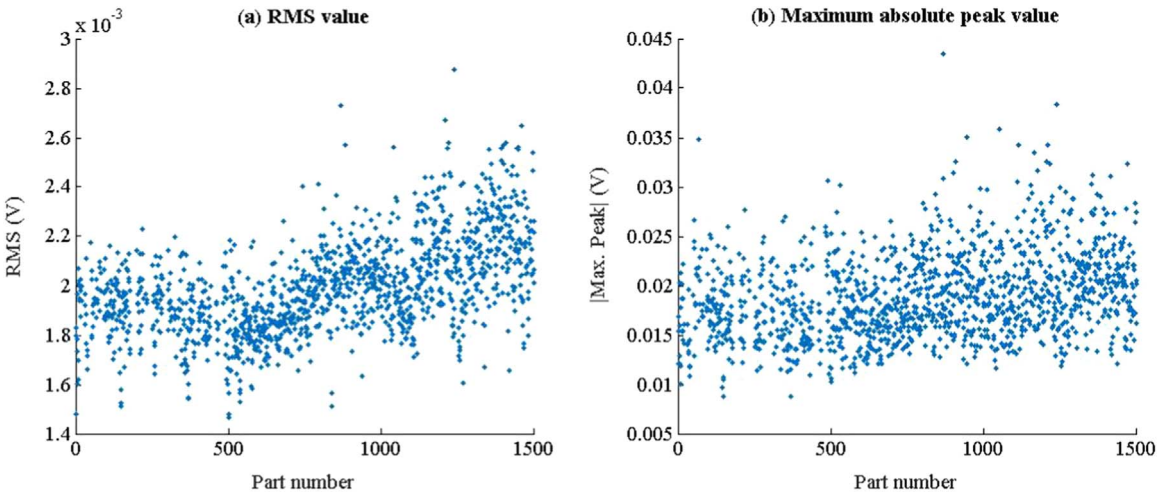


**Fig. 10.** Time domain features of the extracted audio waveform corresponding to the formed channel parts (1–1500) (a) RMS value (b) maximum absolute peak amplitude.

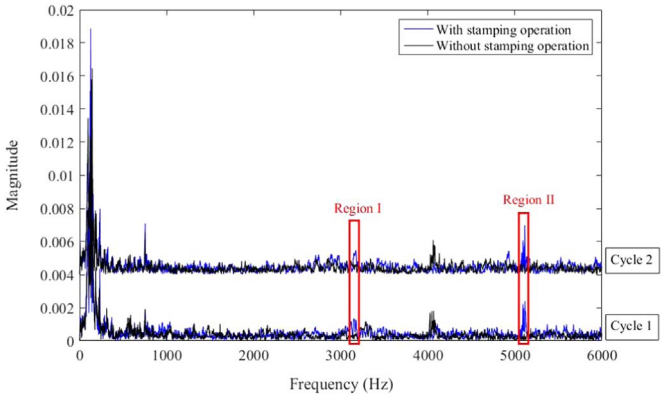


**Fig. 11.** The frequency distribution of emitted audio for two consecutive cycles: with and without stamping operation.

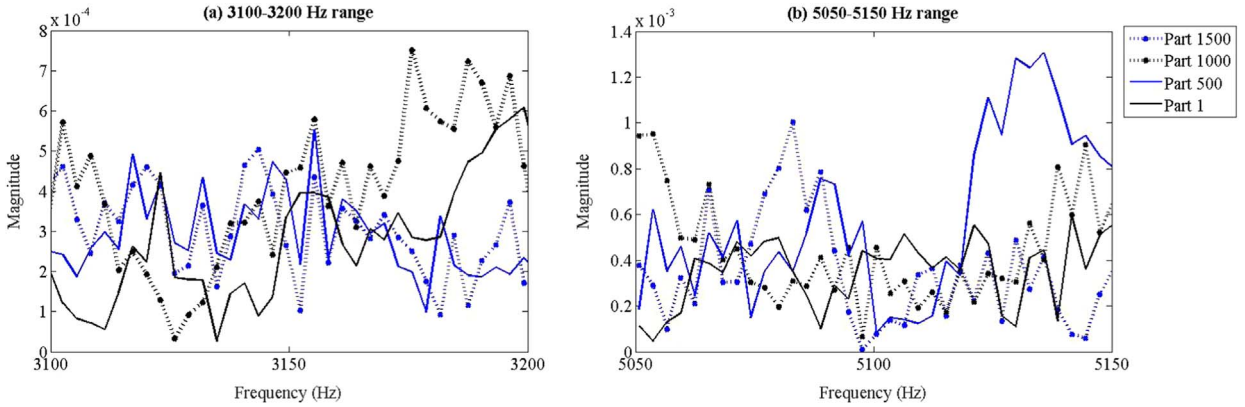


**Fig. 12.** The frequency distribution of four selected parts (Part 1, Part 500, Part 1000, Part 1500) of audio signals within the designated frequency regions (a) 3100–3200 Hz and (b) 5050–5150 Hz.

stamping operation and to continue the analysis to study the magnitude at the excited frequency for all formed parts.

Raja et al. [28] constructed Hilbert Spectra using the intrinsic mode functions (IMF), obtained using empirical mode decomposition (EMD), of the emitted sound by a machining operation. They showed an increasing pattern from fresh, to slightly worn to severely worn tools. The similar analysis was conducted on the emitted audio data by the stamping press in the current study. The time domain projection of the Hilbert Spectra of the seven selected parts are demonstrated in Fig. 13, where it is evident that those results failed to show any trend with the wear progression.

Ge et al. [50] used frequency band energy (FBE) of wavelet packets as the feature for condition monitoring. The FBE coefficients for audio signals associated with stamping operation are presented in Fig. 14. Since, frequency bands 1–5 displayed some decreasing trend with the wear progression, the total energy within these bands was studied for all the stamped parts, and the results are presented in Fig. 15. The result shows a decreasing trend, but there are higher fluctuations compared to the spectral analysis results presented in Figure 7.

The existing works [28,49,50] failed to exploit a significant correlation between the continuous wear progression and the emitted audio because those techniques are not designed to deal with the signals which are highly contaminated by noise. Furthermore, the time domain features previously used by the authors [25], which was capable of distinguishing few distinct wear/process conditions, failed to show a significant correlation when analysing continuous wear progression. Compared to these existing works, the authors' novel approach demonstrates a more significant correlation between wear progression and the emitted audio.

## 5. Discussion

This study has identified that there is a significant qualitative correlation between the progressive wear conditions of stamping dies and the emitted audio signature during the stamping operation. To the authors' knowledge, this is the first study of its kind to use audio sensor signals for progressive tool wear analysis of the stamping process. Although other signal types – including tonnage, acceleration, and acoustic emission – have been examined previously, audio may be a preferred alternative over other sensor types that can be more expensive and more difficult in their placement and implementation for complex stamping setups.

Audio signal analysis has been researched for other manufacturing operations based on distinguishing the process conditions via

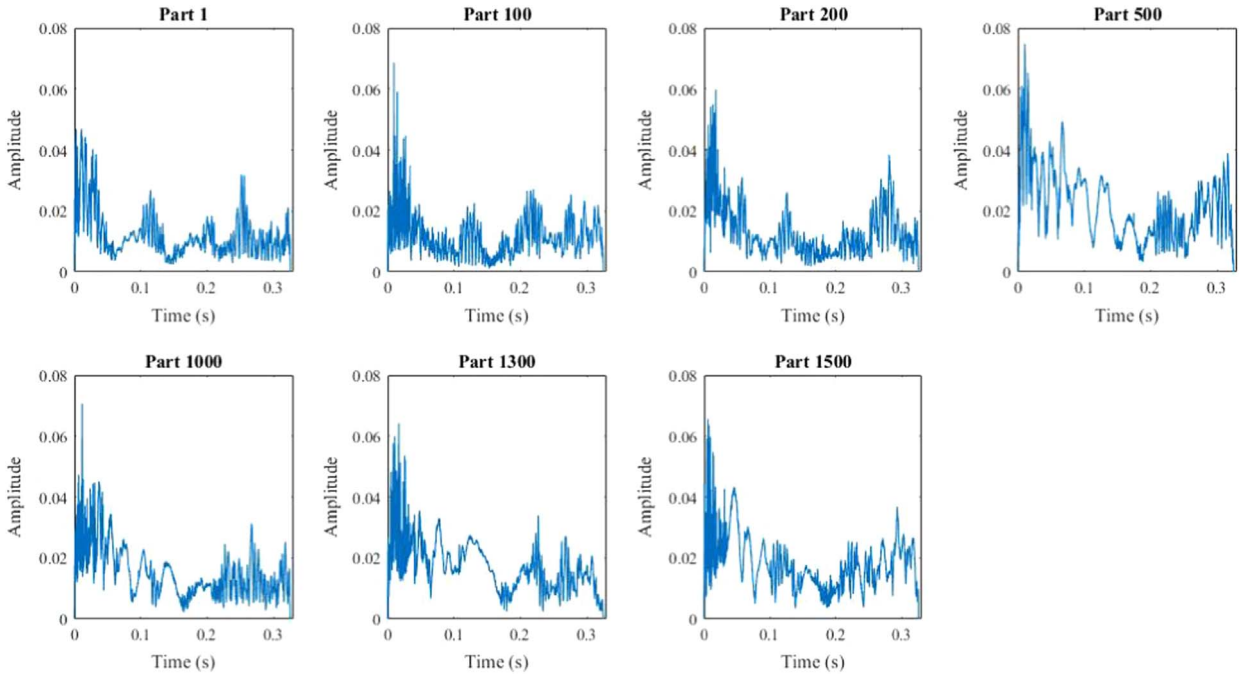


**Fig. 13.** Time domain projections of Hilbert Spectra of audio signals associated with selected parts.

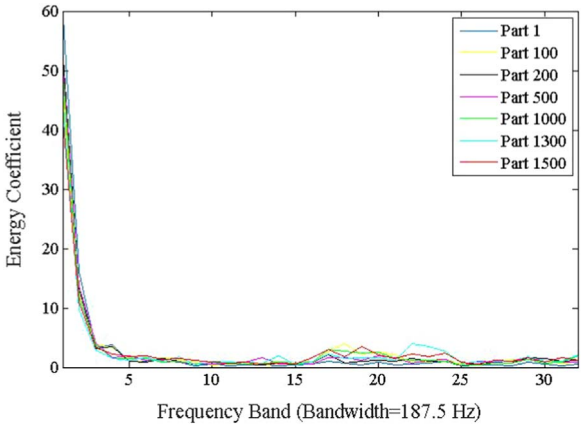


**Fig. 14.** Frequency band energy of audio for selected parts.

the change in sound that can be heard by the human ear [32]. In this study on sheet metal stamping, the sound does not have a difference which is perceptible to human hearing. However, a significant difference was judged in the frequency spectra between the worn and unworn conditions of the die. From the research findings of other manufacturing operations, it is evident that signal behaviour is different from application to application. In this study, an increase in the signal power was observed with the wear progression of stamping tools. Furthermore, the frequency band of 2–6 kHz can be identified as the richest with wear related information in this sheet metal stamping application.

From the aggregate power analysis, the most rapid increase in RCSPI was observed after approximately 500 parts were stamped, corresponding to the point where the scratches due to wear became severe at the edge, but had not yet spread to the middle of the sidewalls. Identification of wear formation at this stage has the potential to allow forecasting of the tool lifespan so that precautions or preventative maintenance can be conducted prior to die failure, thus preventing unscheduled production downfalls. Hence, this approach provides a vital step towards bridging the gap between existing techniques, which are capable of detecting only severe tool wear or tool breakage, and the requirement of detecting the onset of wear. This is especially important for industries like the automobile industry, where the maintenance of a high level of surface quality is critical. For example, for outer-body automobile panels, even very minor wear on the tool surfaces can result in unacceptable product quality. Hence, the focus of future research will be on the emitted audio signal behaviour even before the scratches can be visually observed at the edges of the sidewalls, since the identification of the wear formation at the earliest stage is the primary intention of any future condition monitoring system. The

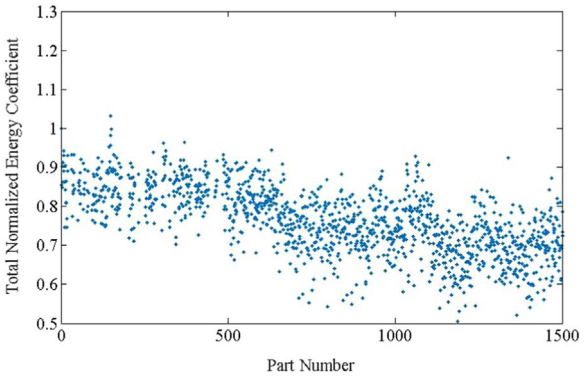


**Fig. 15.** The total normalized energy of audio within the 1–5 frequency bands.

analysis of the raw microphone outputs displays the increment of the spectral magnitudes from low wear conditions to severe wear conditions. However, the extracted signals show a more gradual increment at each step of the selected parts. This is because the overall stamping operation is a complex composite of several processes such as feeding, piercing, trimming, etc., and the signal extraction technique alleviates the contribution of the other processes, recovering the audio signal associated with stamping only. The increasing trend in the aggregate spectral indices is significant even without the application of the signal extraction because the background conditions are less complex in this experiment. All other processes, except for the stamping operation which experienced wear at the die radius, were kept as constant as possible. That is, all other tools were not changed for the duration of the tests, and the wear on the piercing and trimming punches are insignificant over the trial period, due to very low wear rates that correspond to the tool life for these components in excess of 200,000 pieces formed. The sheet material was fed from the same coil, and the same lubrication method was used throughout the operation. However, real applications may have more complex environments [51], where other sound generating mechanisms can vary during the data collection. Hence, the signal extraction may be essential to distinguish changes in the audio emitted by the stamping die due to wear progression.

Four of the existing condition monitoring approaches were tested on the audio data emitted by the stamping operation of the current study. These methods failed to reveal a significant pattern between the selected feature and the wear formation. The reason is either that: they were not capable of directly identifying the wear related information when the sources are highly corrupted; or they had a scope limited to the detection of only few distinct wear levels.

The semi-blind signal extraction technique could not be evaluated alone because it is impractical to collect the benchmark audio signal corresponding to the stamping operation alone. The reason behind this is that it is impossible to run the stamping operation alone without piercing and trimming operations, due to the mechanical nature, geometry and safety conditions of the stamping press. This was the primary motivation for the development of the semi-blind signal extraction technique. In addition, it should be noted that the signal extraction technique employed here is not a complete solution, and the purpose of this study was first to investigate the eligibility of audio signals for wear progression detection.

The significant correlation between wear progression and the audio signals found in this analysis ensures the future research direction of condition monitoring based on more straightforward and inexpensive audio analysis. The semi-blind signal extraction technique isolates the stamping operation, which was not physically feasible otherwise. This enabled the study of the original signal characteristics of the emitted audio. Future research will be focused on the development of new blind signal separation techniques based on these original signal characteristics. These future blind signal separation techniques could be applicable to general stamping operations because we can expect the original signal characteristics of the audio emitted by stamping operations to be common, due to the similarity in geometry and mechanics. In addition, the proposed blind signal extraction could be a potential approach to other manufacturing processes, whose signals are contaminated by noise.

In addition, the frequency analysis conducted in this study demonstrated a significant qualitative correlation between wear formation and the emitted audio. The experimental design closely replicated the geometric, process and material parameters of industrial stamping operations and near-production process conditions. The emphasis was given to the wear conditions at the die radii, which are commonly witnessed in automotive sheet metal stamping. Due to this similarity, the audio-based wear progression indicator could be generalized to other industrial stamping presses as well.

## 6. Conclusion

In this paper, experiments were conducted to study the emitted sound behaviour during the wear progression of stamping tools. Spectral analysis and the aggregate power analysis were conducted on raw and extracted audio signals using semi-blind signal extraction techniques.

The key findings of this research and their significance are summarized below:

1. A semi-blind signal separation algorithm has been employed to allow the audio signal of the stamping operation to be recovered from the mixed signals from the other processes, such as feeding, clamping, piercing, trimming, etc., under realistic stamping

process conditions.

2. The audio signals have a significant qualitative correlation with the tool wear progression during sheet metal stamping process. This trend was observed with and without signal pre-processing. To the authors' best knowledge, this is the first time audio analysis has been correlated to the progression of wear of stamping dies. This is particularly significant because changes in the sound from the stamping operation are not perceptible to human hearing.
3. After the signal extraction data analysis techniques were applied, the increasing trend of the magnitude of the frequency spectra were more obvious when compared to the raw signal analysis. Therefore, the employment of a blind signal extraction technique may be vital in a more complex environment, where there are potentially numerous causes for changing audio emissions, thus making it difficult to distinguish the contribution associated with stamping die wear.
4. The frequency band of 2–6 kHz was identified as containing the most important wear-related information in this sheet metal stamping application. This knowledge will allow future studies to focus on these signals for the identification of the wear state of the stamping process.
5. The increment in the band power of the stamping signal is noticeable at an early stage before the wear has become severe, and significantly prior to the failure of the process. This behaviour may form the basis for the development of a real-time tool condition monitoring system, since the intended system should aim to identify wear formation before it is severe enough to cause production downfall.

## Acknowledgments

This research was supported by an Australian Research Council (Australia) Linkage Project (LP120100239) and the Ford Motor Company University Research Program (URP Number: 2010-4003R). The authors would like to thank Dr. Hamid Abdi and Dr. Harisankar Parippaayillam for their contribution in the data acquisition system development.

## References

[1] Ö.N. Cora, M. Koç, Experimental investigations on wear resistance characteristics of alternative die materials for stamping of advanced high-strength steels (AHSS), Int. J. Mach. Tools Manuf. 49 (2009) 897–905.
[2] R. Du, Y.S. Xu, A review on the sensing and on-line monitoring of sheet metal stamping operations, Proceedings of the 5th International Conference on Frontiers of Design and Manufacturing (ICFDM'02), 2002, pp. 412-420
[3] R. Aronson, Intelligent presses, Manuf. Eng. 121 (1998).
[4] T. Beard, New force in stamping process control, Mod. Mach. Shop 61 (1989) 66–75.
[5] G. Brueninghaus, Process monitoring in the sheet metal processing industry, VDI-Z. 130 (1988) 99–101.
[6] G. Brueninghaus, Process supervision of automatic stamping presses, Wire 44 (1994) 130–135.
[7] D. Xu, E. Liasi, W. Guo, R. Du, Visual comparison of multiple tonnage signatures by using snake skeleton graph, Mech. Syst. Signal Process. 19 (2005) 311–328.
[8] M. Doolan, S. Kalyanasundaram, M. Cardew-Hall, P. Hodgson, Use of image recognition techniques in the analysis of sheet metal forming force signature curves, J. Manuf. Sci. Eng. 125 (2003) 363–368.
[9] G.C. Zhang, M. Ge, H. Tong, Y. Xu, R. Du, Bispectral analysis for on-line monitoring of stamping operation, Eng. Appl. Artif. Intell. 15 (2002) 97–104.
[10] E. Doege, F. Meiners, T. Mende, W. Strache, J.W. Yun, sensors for process monitoring: metal forming, Sens. Appl. (2008) 172–202.
[11] S. Hao, S. Ramalingam, B.E. Klamecki, Acoustic emission monitoring of sheet metal forming: Characterization of the transducer, the work material and the process, J. Mater. Process. Technol. 101 (2000) 124–136.
[12] T.H. Chen, M.C. Lu, S.J. Chiou, C.Y. Lin, M.H. Lee, Study of sound signal for tool wear monitoring system in micro-milling processes, Proceedings of the ASME International Manufacturing Science and Engineering Conference 2009 (MSEC'09), 2009, pp. 57-65
[13] A. Albarbar, F. Gu, A.D. Ball, Diesel engine fuel injection monitoring using acoustic measurements and independent component analysis, Meas.: J. Int. Meas. Confed. 43 (2010) 1376–1386.
[14] Y. Wang, Y. Chi, X. Wu, C. Liu, Extracting acoustical impulse signal of faulty bearing using blind deconvolution method, Proceedings of the 2nd International Conference on Intelligent Computation Technology and Automation (ICICTA'09), 2009, pp. 590-594
[15] M.C. Lu, E. Kannatey-Asibu Jr, Analysis of sound signal generation due to flank wear in turning, J. Manuf. Sci. Eng. Trans. ASME 124 (2002) 799–808.
[16] D.R. Salgado, F.J. Alonso, An approach based on current and sound signals for in-process tool wear monitoring, Int. J. Mach. Tools Manuf. 47 (2007) 2140–2152.
[17] A. Samraj, S. Sayeed, J.E. Raja, J. Hossen, A. Rahman, Dynamic clustering estimation of tool flank wear in turning process using SVD models of the emitted sound signals 80, World Academy of Science, Engineering and Technology, 2011, pp. 1322–1326.
[18] M.-C.L.a.J.-C.T. Ming-Hsing Lee, Development of sound based tool wear monitoring system in micro-milling, ASME 2010 International Manufacturing Science and Engineering Conference, Erie, Pennsylvania, USA, 2010, pp. 8
[19] V. Schulze, P. Weber, C. Ruhs, Increase of process reliability in the micro-machining processes EDM-milling and laser ablation using on-machine sensors, J. Mater. Process. Technol. 212 (2012) 625–632.
[20] E.D. Eneyew, M. Ramulu, On-line monitoring of drill wear using air-coupled audio microphone when drilling composite materials, Appl. Mech. Mater. 590 (2014) 645–650.
[21] E.D. Eneyew, M. Ramulu, Tool wear monitoring using microphone signals and recurrence quantification analysis when drilling composites, Adv. Mater. Res. (2013) 239–244.
[22] J. Downey, P. O'Leary, R. Raghavendra, Comparison and analysis of audible sound energy emissions during single point machining of HSTS with PVD TiCN cutter insert across full tool life, Wear 313 (2014) 53–62.
[23] S. Takata, J.H. Ahn, M. Miki, Y. Miyao, T. Sata, A Sound monitoring system for fault detection of machine and machining states, CIRP Ann. - Manuf. Technol. 35 (1986) 289–292.
[24] H. Trabelsi, E. Kannatey-Asibu Jr, Pattern-recognition analysis of sound radiation in metal cutting, Int. J. Adv. Manuf. Technol. 6 (1991) 220–231.
[25] I. Ubhayaratne, Y. Xiang, M. Pereira, B. Rolfe, An audio signal based model for condition monitoring of sheet metal stamping process, Proceedings of the 10th IEEE Conference on Industrial Electronics and Applications (ICIEA'15), Auckland, New Zealand, 2015
[26] V. Manoj, K. Gopinath, G. Muthuveerappan, A combined approach for condition monitoring of steel rollers using vibration, sound and wear particle analysis, Proceedings of the 12th National Conference on Machines and Mechanisms (NaCoMM'05), 2005, pp. 183-188
[27] E.R. Joseph, L.C. Kiong, L.W. Soong, S. Purushothaman, Emitted sound amplitude analysis using Hilbert Huang transformation for cutting tool flank wear prediction, Glob. Trends Comput. Commun. Syst. (2012) 743–752.

[28] J.E. Raja, L.C. Kiong, L.W. Soong, Hilbert–Huang transform-based emitted sound signal analysis for tool flank wear monitoring, Arab. J. Sci. Eng. 38 (2013) 2219–2226.
[29] R.G. Silva, R.L. Reuben, K.J. Baker, S.J. Wilcox, Tool wear monitoring of turning operations by neural network and expert system classification of a feature set generated from multiple sensors, Mech. Syst. Signal Process. 12 (1998) 319–332.
[30] K. Abed-Meraim, W. Qiu, Y. Hua, Blind system identification, Proc. IEEE 85 (1997) 1310–1322.
[31] Y. Xiang, Blind source separation based on constant modulus criterion and signal mutual information, Comput Electr Eng 34 (2008) 416–422.
[32] Y. Xiang, W. Yu, J. Zhang, S. An, Blind source separation based on phase and frequency redundancy of cyclostationary signals, IEICE Trans. Fundam. Electron. Commun. Comput. Sci. E87-A (2004) 3343–3349.
[33] D. Peng, Y. Xiang, Underdetermined blind separation of non-sparse sources using spatial time-frequency distributions, Digit. Signal Process.: Rev. J. 20 (2010) 581–596.
[34] P. Comon, C. Jutten, Handbook of Blind Source Separation: Independent component analysis and applications, first ed., Academic press, 2010.
[35] R. Boustany, J. Antoni, Blind extraction of a cyclostationary signal using reduced-rank cyclic regression—a unifying approach, Mech. Syst. Signal Process. 22 (2008) 520–541.
[36] R. Boustany, J. Antoni, A subspace method for the blind extraction of a cyclostationary source: Application to rolling element bearing diagnostics, Mech. Syst. Signal Process. 19 (2005) 1245–1259.
[37] N. Bouguerriou, M. Haritopoulos, C. Capdessus, L. Allam, Novel cyclostationarity-based blind source separation algorithm using second order statistical properties: theory and application to the bearing defect diagnosis, Mech. Syst. Signal Process. 19 (2005) 1260–1281.
[38] H. Shao, X. Shi, L. Li, Power signal separation in milling process based on wavelet transform and independent component analysis, Int. J. Mach. Tools Manuf. 51 (2011) 701–710.
[39] X. Shi, R. Wang, Q. Chen, H. Shao, Cutting sound signal processing for tool breakage detection in face milling based on empirical mode decomposition and independent component analysis, J. Vib. Control 21 (2015) 3348–3358.
[40] Y. Sun, Y. Liu, Z. Yu, H. Yu, J. Xu, Milling force mixed-signal denoising based on ICA in high speed micro-milling, Proceedings of IEEE International Conference on Robotics and Biomimetics (ROBIO'12) - Conference Digest, 2012, pp. 1023-1028.
[41] M.P. Pereira, W. Yan, B.F. Rolfe, Sliding distance, contact pressure and wear in sheet metal stamping, Wear 268 (2010) 1275–1284.
[42] M.P. Pereira, M. Weiss, B.F. Rolfe, T.B. Hilditch, The effect of the die radius profile accuracy on wear in sheet metal stamping, Int. J. Mach. Tools Manuf. 66 (2013) 44–53.
[43] L.N.L. De Lacalle, A. Lamikiz, J. Sánchez, J. Arana, Improving the surface finish in high speed milling of stamping dies, J. Mater. Process. Technol. 123 (2002) 292–302.
[44] M.P. Pereira, W. Yan, B.F. Rolfe, Wear at the die radius in sheet metal stamping, Wear 274–275 (2012) 355–367.
[45] M. Liljengren, K. Kjellsson, D. Wiklund, Improved nodular iron for forming dies to obtain functional die surfaces, Proceedings of IDDRG 2008 Conference, Olofström, Sweden, 2008, pp. 615-626.
[46] V.I. Inc., Dektak 8 Advanced Development Profiler Manual, Software Version 8.35, 980-273 (standard),980-271 (cleanroom), Veeco Instruments, Inc., United States of America. Accessed 2016.06.29. ⟨https://www.utdallas.edu/~gpp052000/Docs/Dektak8_Manual.pdf⟩.
[47] Y. Xiang, S.K. Ng, An approach to nonirreducible MIMO FIR channel equalization, IEEE Trans. Circuits Syst. II: Express Briefs 56 (2009) 494–498.
[48] M. de Rooij, D. Schipper, Analysis of material transfer from a soft workpiece to a hard tool: Part I—Lump growth model, J. Tribology 123 (2001) 469–473.
[49] D.Y. Sari, T.-L. Wu, B.-T. Lin, Preliminary study for online monitoring during the punching process, Int. J. Adv. Manuf. Technol. (2016) 1–11.
[50] M. Ge, G.C. Zhang, R. Du, Y. Xu, Feature extraction from energy distribution of stamping processes using wavelet transform, J. Vib. Control 8 (2002) 1023–1032.
[51] Y. Xiang, I. Ubhayaratne, Z. Yang, B. Rolfe, D. Peng, Blind extraction of cyclostationary signal from convolutional mixtures, Proceedings of the 9th IEEE Conference on Industrial Electronics and Applications (ICIEA'14), 2014, pp. 857-861.